

# Design of a Dynamic Additive Manufacturing System for Use on Free-Moving Human Anatomy<sup>1</sup>

**Anna French**

Department of Mechanical Engineering,  
University of Minnesota,  
Minneapolis, MN 55455

**John O'Neill**

Department of Mechanical Engineering,  
University of Minnesota,  
Minneapolis, MN 55455

**Timothy M. Kowalewski**

Department of Mechanical Engineering,  
University of Minnesota,  
Minneapolis, MN 55455

## 1 Background

Bioprinting is an emerging field that has advanced the process of tissue engineering using 3D printing technology. In situ bioprinting has been investigated at other institutions, wherein the tissue is printed cell-by-cell directly onto the site of interest [1,2]. However, these printing systems assumed rigid and fixtured target anatomy. In situations such as printing onto a moving hand, a pulsing blood vessel or a beating heart, this assumption cannot be met. This investigation demonstrates the design process for the robotic linkage of a printing system that can track and print on moving anatomy.

Prior attempts at tracking and drawing on a hand used a commercial robotic arm [3]. This solution was expensive, bulky and unsafe for the task. It is shown here that an inexpensively manufactured two-link robotic arm that is kinematically optimized for hand motion can deliver the necessary torque and speed to track a hand. This kinematic optimization can be performed using tracked hand data, and the results of this optimization method are outlined below.

## 2 Methods

The objective was to create a low cost robot to track human hand motion. To minimize cost and complexity for the purpose of this investigation, the hand is only tracked in two degrees-of-freedom in a plane parallel to the ground. These assumptions lead to a two link, revolute jointed serial robot design.

**2.1 Hardware Design.** Tracked hand data was initially unavailable for the design process, so link lengths for the planar arm were optimized to minimize length while still meeting the requirements of tracking a human hand over a workspace of a 50 mm square. The manipulability was assessed to perform this optimization, which is a number measuring the ability of the end effector to move in any given direction. The manipulability is a function of the Jacobian and is thus specific to a given configuration of the robot arm, i.e., a given  $\theta_1$  and  $\theta_2$ . The Jacobian is a matrix that can be used to translate the motor angular velocities into tool tip planar velocity.

To bound the worst case effective radius, the minimum singular value decomposition was chosen as the metric of manipulability. The singular value decomposition of the Jacobian yields two

values, and this analysis is only interested in the smaller of the two values,  $\sigma_{\min} = \min(\text{svd}(\mathbf{J}))$ . Placing a bound on this value can ensure that the velocity requirement is satisfied in any direction. This is equivalent to placing the tool tip in a given start position and finding the maximum speed the tool tip can move in any given direction from this start position, then picking the slowest observed speed and direction and maximizing that minimum speed by varying the link lengths. To achieve the desired kinematics, a minimum effective radius was found to be  $r_{\min} = 159$  mm. The minimum effective radius was set using the relationship  $V = \omega * r$ , where the  $r$  is the minimum effective radius and is found by dividing the desired speed of (here,  $V = 1$  m/s was used to demonstrate the process) by the maximum angular velocity of the motor  $\omega = 60$  rpm.

A bisection search was used to determine the optimal link lengths—minimizing the total length, while still ensuring the desired manipulability is met. At each iteration, the manipulability metric was calculated over a grid in joint angle space. Using forward kinematics, this was then converted to a grid in Cartesian space. If the predetermined minimum value was not achieved inside a 50 mm square, then the link lengths were increased by a fixed amount. If it was achieved, then the link lengths were decreased by half the previous increase (bisection method). This allowed the minimum total link lengths that meet the manipulability metric to be found.

The square workspace was centered along the  $x$  axis at  $(L1 + L2)/2$ . The optimal link lengths were found to be  $L1 = 228$  mm and  $L2 = 228$  mm. The manipulability for the optimized linkage over a portion of its workspace is displayed in Fig. 1. The central band (lighter color) region shows the where the effective radius is at an acceptable length for our requirements (where it is at least the minimum effective radius). The 50 mm  $\times$  50 mm square shows that we have acceptable manipulability in our target region size for our chosen  $L1$  and  $L2$ .

Figure 2 shows a solid model rendering of the designed robot. The planar arm is constructed of a laser-cut pattern of 6 mm cast

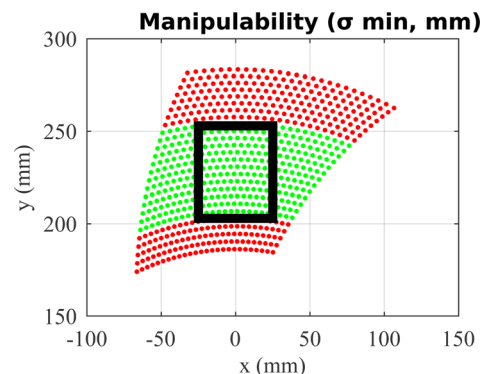


**Fig. 1 Manipulability of planar arm over its workspace. The central band (lighter color) defines the region where  $\sigma_{\min} > r_{\min}$ .**



**Fig. 2 Solid model rendering of kinematically optimized two-link robot design**

<sup>1</sup>Accepted and presented at The Design of Medical Devices Conference (DMD2016), April 11–14, 2016, Minneapolis, MN, USA.

DOI: 10.1115/1.4033171

Manuscript received March 1, 2016; final manuscript received March 17, 2016; published online May 12, 2016. Editor: William Durfee.

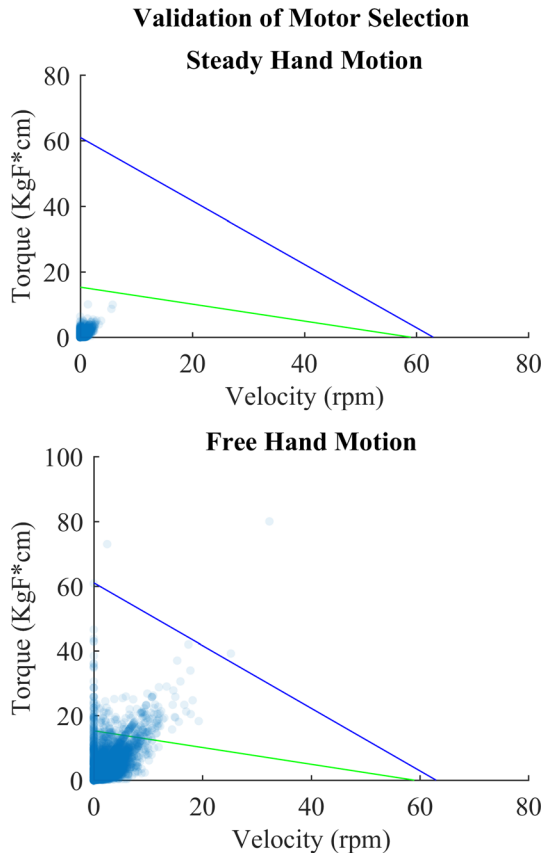


**Fig. 3 Torque-speed curves of candidate motors plotted against moving hand scatter plot data from leap motion sensor. Upper curve is MX-64 motor, lower curve MX-12.**

acrylic, with Dynamixel MX-64T servomotors (ROBOTIS Ltd., Seoul, South Korea) servo motors.

### 3 Results

The torque-speed curves for two candidate motors are displayed in Fig. 3. These torque-speed curves are compared against sample

hand motion data, which is overlaid as scatter plot data. This hand motion data was gathered by recording the position and velocity of a hand using the Leap Motion sensor. Two different hand motion regimes were recorded. Under the steady hand motion type, the subject attempted to hold their hand as stationary as possible for 60 s. The recorded data reported an average speed of 6 mm/s for the center of mass of the hand and covered an area of 112 mm<sup>2</sup>. Under the free hand motion type, the movement is greater, with an average speed of 40 mm/s and varying over 8400 mm<sup>2</sup>.

The discrete points of sampled position and velocity data from the leap motion were translated into the torque and velocity from the motors required to keep the tool tip of the two-link arm coincident on the center of mass of the hand. This calculation was performed by simplifying the arm model as a point mass located at  $r_{min}$ .

Figure 3 shows that the MX-12 motor delivers acceptable torque and speed under steady hand motion, but the increased torque provided by the MX-64 is required to track free hand motion.

### 4 Interpretation

This work demonstrates that a robotic linkage can be designed to meet the kinematic and dynamic requirements to match typical human motion in a predetermined workspace. While the analysis was limited to a two-link serial robot, it can extend to multiple degrees of freedom and to parallel mechanisms. Future work will extend this approach to a delta robot—a parallel mechanism with more degrees of freedom—and aim to include tracking of 3D hand motion or respiratory motion near the chest.

### References

- [1] Binder, K. W., Zhao, W., Aboushwareb, T., Dice, D., Atala, A., and Yoo, J. J., 2010, "In Situ Bioprinting of the Skin for Burns," *J. Am. Coll. Surg.*, **211**(3), p. S76.
- [2] Institute for Regenerative Medicine, "Printing Skin Cells on Burn Wounds," Wake Forest School of Medicine, Winston-Salem, NC, accessed Jan. 26, 2016, <http://www.wakehealth.edu/Research/WFIRM/Research/Military-Applications/Printing-Skin-Cells-On-Burn-Wounds.htm>
- [3] O'Neill, J. J., and Kowalewski, T. M., 2014, "Online Free Anatomy Registration Via Noncontact Skeletal Tracking for Collaborative Human/Robot Interaction in Surgical Robotics," *ASME J. Med. Devices*, **8**(3), p. 030952.